

# Implicit and Explicit Language Guidance for Diffusion-based Visual Perception

Hefeng Wang, Jiale Cao, Jin Xie, Aiping Yang, and Yanwei Pang

**Abstract**—Text-to-image diffusion models have shown powerful ability on conditional image synthesis. With large-scale vision-language pre-training, diffusion models are able to generate high-quality images with rich texture and reasonable structure under different text prompts. However, it is an open problem to adapt the pre-trained diffusion model for visual perception. In this paper, we propose an implicit and explicit language guidance framework for diffusion-based perception, named IEDP. Our IEDP comprises of an implicit language guidance branch and an explicit language guidance branch. The implicit branch employs frozen CLIP image encoder to directly generate implicit text embeddings that are fed to diffusion model, without using explicit text prompts. The explicit branch utilizes the ground-truth labels of corresponding images as text prompts to condition feature extraction of diffusion model. During training, we jointly train diffusion model by sharing the model weights of these two branches. As a result, implicit and explicit branches can jointly guide feature learning. During inference, we only employ implicit branch for final prediction, which does not require any ground-truth labels. Experiments are performed on two typical perception tasks, including semantic segmentation and depth estimation. Our IEDP achieves promising performance on both tasks. For semantic segmentation, our IEDP has the mIoU<sup>SS</sup> score of 55.9% on AD20K validation set, which outperforms the baseline method VPD by 2.2%. For depth estimation, our IEDP outperforms the baseline method VPD with a relative gain of 10.2%.

**Index Terms**—Diffusion model, language guidance, visual perception

## I. INTRODUCTION

Diffusion models have exhibited exceptional performance in the related field of image synthesis [1]–[3], which can recover high-quality images from noisy data. To reduce the significant training cost in pixel space, stable diffusion model [4] has been proposed to perform diffusion forward and reverse backward on feature latent space. Through training on large-scale image-text paired dataset LAION-5B [5], stable diffusion model can generate various high-quality images with rich texture and reasonable structure under various text prompts. This phenomenon suggests that stable diffusion model has the strong feature representation ability of both low-level and high-level semantic information.

Recently, the researchers [6], [7], [10] started to explore diffusion model for visual perception via fully utilizing its strong feature representation ability. VPD [6] first generates

H. Wang, J. Cao, A. Yang, and Y. Pang are with the School of Electrical and Information Engineering, Tianjin University, Tianjin 300072, China, also with Shanghai Artificial Intelligence Laboratory, Shanghai 200232, China (E-mail: {wanghefeng, connor, yangaiping, pyw}@tju.edu.cn).

J. Xie is with the School of Big Data and Software Engineering, Chongqing University, Chongqing 401331, China (E-mail: xiejin@cqu.edu.cn).

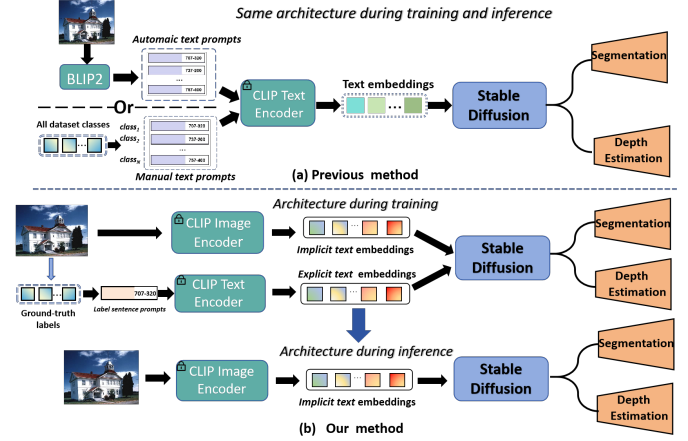


Fig. 1. Comparison between existing methods and our proposed method. In (a), the existing methods [6], [7] first employ all dataset classes or BLIP-2 [8] model to manually or automatically generate text prompts, and then utilize frozen CLIP [9] text encoder to extract text embeddings, which are fed to stable diffusion to condition feature extraction. During training and inference, these methods adopt the same structure. In (b), our proposed method introduces two branches to generate implicit and explicit text embeddings for stable diffusion during training, where these two branches can jointly train the model. During inference, we only employ implicit branch to generate implicit text embeddings for perception tasks.

text prompts with all semantic classes existing in the dataset, and then utilizes these text prompts to condition feature extraction of stable diffusion. VPD has exhibited promising performance on various perception tasks, especially when using fewer training iterations. However, VPD employs all semantic classes from the entire dataset, which does not align the specific image that only contains several classes. To address this issue, TADP [7] adopts the pre-trained vision-language model BLIP-2 [8] to generate image-aligned captions, and employs these image-aligned captions to condition feature extraction of diffusion model. Compared to VPD, TADP avoids the interference of non-existing classes when conditioning feature extraction in some degree. We summarize the pipelines of VPD and TADP into Fig. 1(a). They initially rely on manual design or automatic generation to create text prompts. Subsequently, they utilize a CLIP text encoder to extract text embeddings, and fed them into stable diffusion to condition feature extraction. We argue that there exists some limitations in these methods. First, during inference, it is relatively cumbersome in TADP to employ two models to generate text prompts and text embeddings, and there exists a misalignment issue between text prompt and image in VPD. Second, during training, these methods do not fully utilize

ground-truth labels corresponding to specific training images, which accurately align with the training images.

To address these issues above, we propose an implicit and explicit language guidance framework for diffusion-based perception, named IEDP. Our proposed IEDP contains two different branches: implicit language guidance branch and explicit language guidance branch. In the implicit branch, we introduce a novel implicit prompt module that directly generates implicit text embeddings using CLIP image encoder, instead of using explicit text prompts. The implicit text embeddings are fed to stable diffusion to condition feature extraction. Because CLIP model is able to learn connection between image-text pairs, the implicit text embeddings contains class information existing in the image. In the explicit branch, we introduce an explicit prompt module to directly employ ground-truth labels of corresponding training image as explicit text prompts. The ground-truth labels provide accurate class information of the image, which can better guide feature learning. As shown in Fig. 1(b), during training, we jointly train the network via weight sharing between these two branches. During inference, we only employ implicit branch for perception prediction, and remove the explicit branch since the accurate ground-truth labels of test image are not available. We perform the experiments on typical visual perception tasks, including semantic segmentation and depth estimation. The experimental results demonstrate the efficacy of our proposed method. The contributions and merits of our proposed method can be summarized as follows.

- We propose a novel implicit and explicit language guidance framework for diffusion-based perception. The implicit and explicit branches jointly train the model via sharing model weights during training, while only implicit branch is employed during inference.
- In implicit branch, we directly employ frozen image encoder to generate implicit text embeddings to condition feature extraction, which does not require additional model to create explicit text prompts.
- In explicit branch, we employ ground-truth labels of corresponding training image to create text prompts. Compared to automatic text prompts, ground-truth based text prompts are noise-free and can better guide feature learning during training.
- Our method achieves superior performance on semantic segmentation and depth estimation. For example, our IEDP achieves mIoU<sup>ss</sup> score of 55.9% on ADE20K [11] set, outperforming diffusion-based method VPD [6] by 2.2%. On depth estimation, our IEDP achieves RMSE of 0.228 on NYUv2 [12], outperforming VPD by 10.2% relatively.

## II. RELATED WORKS

In this section, we first introduce the related works of visual perception. Afterwards, we give a review on diffusion models. Finally, we introduce diffusion-based visual perception.

### A. Visual Perception

As a typical perception task, semantic segmentation aims to group the pixels in an image into different semantic categories.

In past years, semantic segmentation has achieved remarkable progress, which can be mainly divided into CNN-based and transformer-based approaches. Most CNN-based approaches were developed on fully convolutional framework [13]. To improve segmentation performance, some researchers explored to exploit local contextual information using encoder-decoder [14]–[16] or spatial pyramid structure [17], [18], while some other researchers proposed to exploit non-local contextual information using attention mechanism [19]–[21]. Recently, with the success of transformer in image classification [22], the researchers started to explore transformer-based approaches. Some approaches replace the convolutional backbone with the transformer backbone [23]–[25], while some other approaches design query-based transformer decoder for semantic segmentation [26], [27].

Monocular depth estimation is another fundamental perception task, which plays an important role in 3D vision task. Eigen *et al.* [28] first proposed to employ multi-scale deep features for depth estimation. Afterwards, the researchers proposed many variants for improved depth estimation, such as designing novel model structure [29], [30] and considering geometric constraints [31]–[33].

### B. Diffusion Models

Diffusion models [34]–[37] have exhibited exceptional synthesis quality and controllability in the field of image synthesis. The diffusion model contains a forward diffusion process and a reverse denoising process. The forward diffusion process progressively adds the noise to the image, and the reverse denoising process tends to recover the clean image from the noise. At first, these diffusion models directly operate on pixel space, which require significant training resources and long training time. To address this issue, Rombach *et al.* [4] propose the latent diffusion model (LDM) that performs diffusion on latent feature space, named stable diffusion. Stable diffusion first employs a pre-trained auto-encoder to extract latent feature representation, and then performs diffusion and denoising processes on latent space. Finally, stable diffusion predicts the image from latent space using a decoder. In addition, stable diffusion can condition image synthesis based on texts and semantic maps. Stable diffusion has achieved great success on conditional image synthesis.

### C. Diffusion-based Visual Perception

With the success of diffusion model on image synthesis, the researchers started to employ diffusion models for visual perception. Some researchers explored to extend the diffusion pipeline for visual perception. Chen *et al.* [10] proposed to treat panoptic segmentation as a discrete data generation and employ bit diffusion to predict discrete data. Chen *et al.* [38] introduced diffusion model for object detection by predicting the bounding-boxes from noisy bounding-boxes. Amit *et al.* [39] first extracted deep features from input image and then summed the deep features with noisy segmentation map to condition the denoising process. Ji *et al.* [40] proposed to concatenate the noisy image and deep features to condition

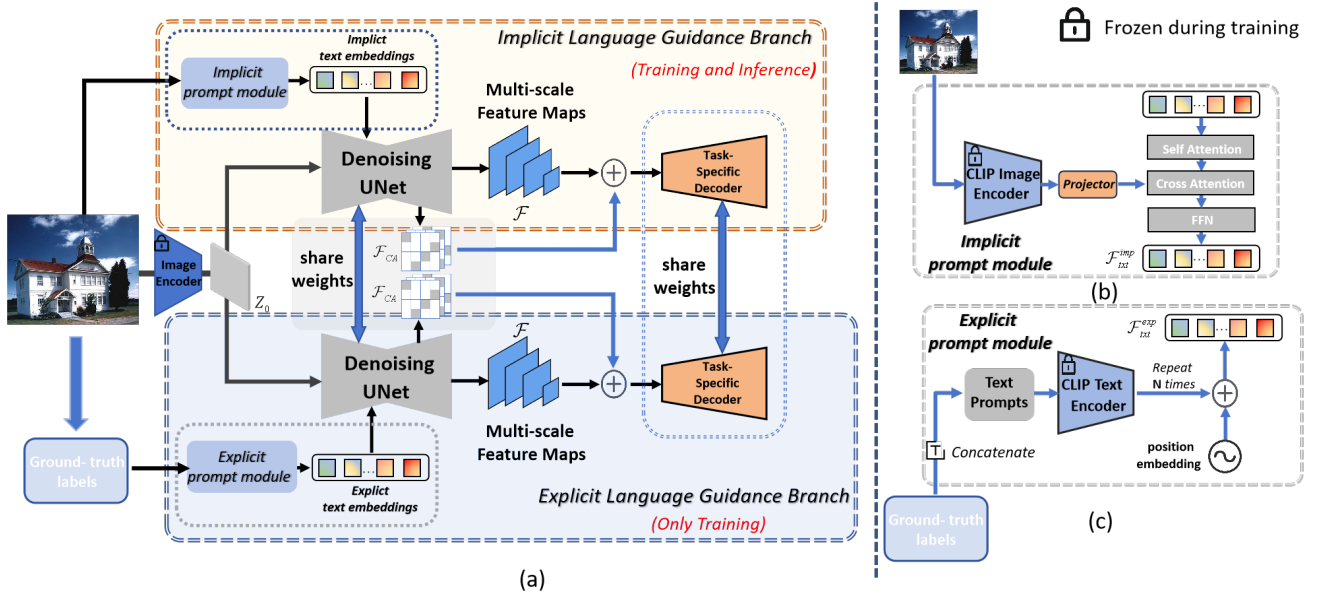


Fig. 2. **Overall architecture of our proposed method.** In (a), we present the overall architecture of our method. We introduce an implicit language guidance branch and an explicit language guidance branch, which respectively utilize the implicit prompt module and explicit prompt module to condition feature extraction of denoising UNet for the following task-specific decoder. These two branches share the weights of model parameters during training. During inference, we only employ the implicit branch. In (b) and (c), we give the detailed structures of implicit prompt module and explicit prompt module.

the denoising process. In addition, some researchers [41] employed diffusion model for label-efficient segmentation.

Instead of using diffusion pipeline, some researchers [6], [7] explored to make full use of the strong feature representation ability of pre-trained diffusion model. These researchers treated diffusion model as a feature extractor. Zhao *et al.* [6] explored to use all dataset classes as text prompts to condition feature extraction of diffusion model, and add a task-specific decoder for visual prediction. Kondapaneni *et al.* [7] argued that using all dataset classes as text prompt can not align the specific image very well. Instead of all dataset classes, Kondapaneni *et al.* [7] proposed to employ BLIP-2 to generate image captions, and condition feature extraction using the generated image captions. However, the proposed method TADP relies on additional network to generate text descriptions during inference. In open-vocabulary panoptic segmentation, Xu *et al.* [42] employed CLIP image encoder to generate text embeddings, named ODISE. Compared to ODISE, our proposed method has following differences: (1) We introduce a novel implicit and explicit language guidance framework, which employs implicit and explicit prompt modules to jointly train the diffusion model for improved visual perception. (2) Compared to ODISE that employs a linear layer to generate text embeddings, our proposed method explores implicit module with learnable queries to extract text embeddings. (3) Instead of open-vocabulary segmentation, our proposed method focuses on classical visual perception tasks.

### III. METHOD

In this section, we introduce our proposed implicit and explicit language guidance framework for diffusion-based visual perception, named IEDP. Following VPD [6], our IEDP employs text-to-image stable diffusion model [4] to fully

utilize its strong feature representation ability. VPD employs all classes existing in dataset as text prompts, resulting in the misalignment with the specific image due to including non-existing classes. Instead of using unaligned text prompts like VPD, our IEDP introduces an explicit prompt module and an implicit prompt module, which both incorporate image-specific semantic information to condition feature extraction. Specifically, the explicit prompt module employs ground-truth labels of corresponding images to extract explicit text embeddings to condition feature extraction of diffusion model. The implicit prompt strategy first employs frozen CLIP image encoder to extract visual features, and then converts these visual features to implicit text embeddings as the input to stable diffusion model.

**Overall architecture.** Fig. 2 presents the overall architecture of our proposed IEDP, integrating our explicit and implicit prompt modules into the base model that contains an image encoder, denoising UNet, and task-specific decoder. Therefore, our IEDP contains two branches: implicit language guidance branch and explicit language guidance branch, which share the weights of model parameters. Given an input image  $I$ , we first employ the image encoder to extract the latent features  $z_0$ , which are then fed to the denoising UNet in both explicit and implicit language guidance branches. In implicit language guidance branch, we employ the implicit prompt module to extract implicit text embeddings  $\mathcal{F}_{txt}^{imp}$  from the input image. Based on implicit text embeddings  $\mathcal{F}_{txt}^{imp}$ , we condition denoising UNet to generate hierarchical feature maps  $\{\mathcal{F}_i, i = 1, 2, 3, 4\}$  and averaged cross-attention feature maps  $\mathcal{F}_{CA}$  similar to VPD. Afterwards, we employ a task-specific decoder for visual prediction. In explicit language guidance branch, we directly utilize the explicit prompt module to generate explicit text embeddings  $\mathcal{F}_{txt}^{exp}$  from the ground-truth

(GT) labels of input image, and condition denoising UNet to generate hierarchical feature maps and averaged cross-attention feature maps. Similar to implicit branch, we perform the prediction with task-specific decoder.

We jointly train the model using both the implicit language guidance branch and explicit language guidance branch. During inference, we only employ implicit branch for prediction, because the ground-truth labels of image are not available, and it is relatively time-consuming to employ two branches for prediction.

### A. Implicit Language Guidance Branch

VPD [6] adopts the unaligned text prompts generated by all dataset classes. Instead of using unaligned text prompts, TADP [7] generates image-aligned text prompts using BLIP-2 generated captions. Based on automatically generated text prompts, TADP further employs a frozen CLIP text encoder to generate text embeddings fed to denoising UNet in stable diffusion model. Though TADP can adaptively generate image-aligned text prompts, we argue that it is relatively cumbersome to employ two networks to generate text prompts and text embeddings respectively. To address this issue, we propose an implicit prompt module to directly generate image-aligned text embeddings from the input image using a single network.

Fig. 2(b) shows the structure of our implicit prompt module. Specifically, we employ frozen CLIP image encoder and a light-weight projector to extract the image visual features  $\mathcal{F}_{vis}$ , which can be written as

$$\mathcal{F}_{vis} = f_{pro}(J_{CLIP}^{img}(I)), \quad (1)$$

where the projector  $f_{pro}$  is an MLP layer. Because CLIP is able to learn the connection between image-text pairs, we believe that the visual features  $\mathcal{F}_{vis}$  implicitly contain semantic information to learn text embeddings. Therefore, we employ a set of learnable queries  $\mathcal{Q}$  to predict implicit text embeddings from the visual features  $\mathcal{F}_{vis}$ . Specifically, we first feed the learnable queries  $\mathcal{Q}$  to a self-attention layer. Then, we perform a cross-attention operation between learnable queries and visual features. Finally, we use an MLP layer to generate implicit text embeddings  $\mathcal{F}_{txt}^{imp}$ . We summarize the detailed process as

$$\begin{aligned} \mathcal{Q}_s &= \mathcal{Q} + f_{SA}(f_{LN}(\mathcal{Q})), \\ \mathcal{Q}_c &= \mathcal{Q}_s + f_{CA}(f_{LN}(\mathcal{Q}_s), f_{LN}(\mathcal{F}_{vis})), \\ \mathcal{F}_{txt}^{imp} &= \mathcal{Q}_c + f_{FFN}(f_{LN}(\mathcal{Q}_c)), \end{aligned} \quad (2)$$

where  $f_{SA}$  is self-attention operation,  $f_{CA}$  is cross-attention operation,  $f_{LN}$  is layer norm operation, and  $f_{FFN}$  is feed-forward layer. We employ  $\mathcal{F}_{txt}^{imp}$  as implicit text embeddings because it is generated from CLIP image encoder, instead of text encoder.

Based on the implicit text embeddings  $\mathcal{F}_{txt}^{imp}$  and the latent features  $z_0$ , we employ denoising UNet to generate hierarchical feature maps and averaged cross-attention map. Similar to VPD, we concatenate these features and feed them to task-specific decoder head for prediction.

### B. Explicit Language Guidance Branch

Compared to unaligned text prompts, the image-aligned text prompts can better condition feature extraction of denoising UNet for visual perception tasks. Though TADP [7] employs BLIP-2 to generate image-aligned text prompts for each image, it is still not very accurate and has noise. In fact, the training image has the corresponding ground-truth class labels, which can be used to generate more accurate text prompts. However, the ground-truth labels of test image are not available. Therefore, it is a natural question, can we only use the accurate ground-truth labels of training images to help improve visual perception model learning during training. Inspired by this, we introduce an explicit prompt module to jointly guide feature learning with implicit branch.

As shown in Fig. 2(c), we first concatenate all ground-truth labels in an image as text prompts  $\mathcal{P}$ , which can be written as

$$\mathcal{P} = \{c + " " | c \in \mathcal{C}_{gt}\}, \quad (3)$$

where  $c$  represents the word of class label, and  $\mathcal{C}_{gt}$  represents the set of all class labels in an image. Then, we feed the text prompts  $\mathcal{P}$  to the frozen CLIP text encoder to generate explicit text embeddings  $\mathcal{F}_{txt}^{exp}$  as

$$\mathcal{F}_{txt}^{exp} = f_{CLIP}^{txt}(\mathcal{P}). \quad (4)$$

To keep the number of explicit text embeddings be consistent with the implicit text embeddings, we repeat the explicit text embeddings. Afterwards, we employ the denoising UNet and task-specific decoder for prediction.

Compared to image-aligned text prompts in TADP, our text prompts are clean and noise-free, which can better guide feature learning. By sharing model weights with implicit branch, the explicit branch is able to jointly affect the feature learning of denoising UNet and task-specific decoder. Moreover, different to TADP, we only employ explicit branch during training, and remove the explicit branch during inference.

### C. Training and Inference

During training, we set the time step  $t$  to be zero, which results in the latent feature map  $z_0$  being noise-free. The hierarchical features  $\mathcal{F}$  can be obtained by extracting the last layer of each decoder block in denoising U-Net, consisting of 4 feature maps of different resolutions. We represent these four feature maps as  $\mathcal{F}_1, \mathcal{F}_2, \mathcal{F}_3, \mathcal{F}_4$ , which has the stride of 8, 16, 32, 64 to the input image. The averaged cross-attention map  $F_{CA}$  are averaged by the cross-attention maps in both encoder and decoder blocks. Afterwards, the hierarchical feature maps and averaged cross-attention map are fed to task-specific decoder to generate the outputs. Finally, we calculate the overall training loss  $L$ , including the implicit loss  $L_{imp}$  and explicit loss  $L_{exp}$  in implicit and explicit branches, which can be written as

$$L = L_{imp} + L_{exp}. \quad (5)$$

The specific implicit loss  $L_{imp}$  and explicit loss  $L_{exp}$  are different for different perception tasks. We use the cross-entropy loss for semantic segmentation task, and the Scale-Invariant loss (SI) [28] for depth estimation.

TABLE I

SEMANTIC SEGMENTATION COMPARISON WITH SOME OTHER METHODS ON ADE20K. THE COMPARED METHODS INCLUDE NON-DIFFUSION-BASED (CLASSICAL) APPROACHES AND DIFFUSION-BASED APPROACHES. COMPARED TO THESE DIFFUSION-BASED APPROACHES, OUR METHOD ACHIEVES A SUPERIOR PERFORMANCE.

Method	Publication	Crop	mIoU <sup>SS</sup>	mIoU <sup>MS</sup>
<i>Non-diffusion-based approaches:</i>				
Swin-L [43]	ICCV'21	640 <sup>2</sup>	52.1	53.5
ConvNeXt-L [44]	CVPR'22	640 <sup>2</sup>	53.2	53.7
ConvNeXt-XL [44]	CVPR'22	640 <sup>2</sup>	53.6	54.0
CLIP-ViT-B [45]	CVPR'22	640 <sup>2</sup>	50.6	51.3
ViT-Adapter [46]	ICLR'23	896 <sup>2</sup>	61.2	61.5
<i>Diffusion-based approaches:</i>				
DDP [40]	ICCV'23	512 <sup>2</sup>	53.2	54.4
VPD [6]	ICCV'23	512 <sup>2</sup>	53.7	54.6
TADP [7]	ArXiv'23	512 <sup>2</sup>	54.8	55.9
<b>IEDP (Ours)</b>	-	512 <sup>2</sup>	55.9	57.1

Our proposed method does not rely on any additional text information during inference, setting it apart from previous methods that use manual text templates or automatic image captions. We directly feed the image to implicit language guidance branch for prediction. Specifically, we use CLIP image encoder to generate implicit text embeddings, and stable diffusion model to generate hierarchical features and cross-attention features, which are fed to a task-specific decoder to generate the final prediction.

#### IV. EXPERIMENTS

In this section, we perform experiments to demonstrate the efficacy and superiority of our proposed method. We evaluate our method on two typical perception tasks, including semantic segmentation and depth estimation.

##### A. Datasets and Evaluation Metrics

**ADE20K.** The ADE20K dataset [11] is a classical semantic segmentation dataset collected from the website. It contains more than 20K natural images with pixel-level annotations. There are totally 150 semantic categories. There are three subsets, including `train`, `val`, and `test-dev` sets. The training set has 20210 images, `val` set has about 2000 images, and the `test` set has about 3000 images. Similar to VPD, we train our method on `train` set and compare with other methods on `val` set. We adopt mIoU as evaluation metric of semantic segmentation.

**NYUv2.** The NYUv2 dataset [12] is a typical depth estimation dataset collected from a variety of indoor scenes. The images and corresponding depth maps are captured by the pairs of RGB and Depth cameras. There are 24k images for training, and 645 images for testing. We adopt three commonly used indicators for depth estimation evaluation, including absolute relative error (REL), root mean squared error (RMSE), and average  $\log_{10}$  error between predicted depth  $\hat{d}$  and ground-truth depth  $d$ . We further present threshold accuracy  $\delta_n$  which represents  $\delta_n = \%$  of pixels satisfying  $\max(d_i/\hat{d}_i, \hat{d}_i/d_i) < 1.25^n$  for  $n = 1, 2, 3$ .

##### B. Experiment Setups

During training, we freeze the image encoder, CLIP image encoder, and CLIP text encoder. Namely, we only fine-tune the denoising UNet and task-specific decoder on four NVIDIA RTX A6000 GPUs. We provide the detailed experiment setups of different tasks as follows.

**Semantic segmentation.** We adopt the semantic FPN as decoder for semantic segmentation as in VPD. During training, we adopt AdamW as the optimizer, and set the batch size as 8. We employ the poly learning rate schedule with a power of 0.9. The initial learning rate is set as 0.00008, and the weight decay is set as 0.001. When comparing with other methods, the number of iterations are 160K. For fast ablation study, the number of iterations are set as 40K. During inference, we perform slide window inference, where the crop window size is  $512 \times 512$  pixels, and the slide stride is  $341 \times 341$  pixels.

**Depth estimation.** We adopt the similar decoder as in [47]. During training, we adopt AdamW as the optimizer, and employ the poly learning rate rate schedule. We randomly crop the images into  $480 \times 480$  pixels, and set the batch size as 24. There are totally 25 epochs. The initial learning rate is  $5e-4$  and the weight decay as 0.1. Because depth estimation dataset does not provide ground-truth labels, we only employ implicit language guidance branch when performing depth estimation. During inference, we employ the techniques of horizontal flipping and sliding windows as in VPD.

##### C. State-of-the-art Comparison

**Semantic segmentation.** We compare our proposed method with some state-of-the-art methods on ADE20K dataset in Table I. These state-of-the-art methods are divided into classical approaches and diffusion-based approaches. We report both the single-scale and multi-scale results for all these approaches. Compared to diffusion-based approaches, our IEDP achieves significant improvement. For instance, VPD has the mIoU<sup>SS</sup> score of 53.7%, while our IEDP has the mIoU<sup>SS</sup> score of 55.9%. Therefore, our IEDP outperforms VPD with an absolute gain of 2.2% on mIoU<sup>SS</sup>. Compared to TADP, our IEDP has 1.1% improvement on mIoU<sup>SS</sup> and 1.2% improvement on mIoU<sup>MS</sup>.

TABLE II  
DEPTH ESTIMATION COMPARISON WITH SOME OTHER METHODS ON NYUv2. THE COMPARED METHODS INCLUDE NON-DIFFUSION-BASED (CLASSICAL) APPROACHES AND DIFFUSION-BASED APPROACHES.

Method	Publication	RMSE↓	$\delta_1 \uparrow$	$\delta_2 \uparrow$	$\delta_3 \uparrow$	REL↓	log10↓
<i>Non-diffusion-based approaches:</i>							
BTS [48]	ArXiv'19	0.392	0.885	0.978	0.995	0.110	0.047
AdaBins [49]	CVPR'21	0.364	0.903	0.984	0.997	0.103	0.044
DPT [50]	ICCV'21	0.357	0.904	0.988	0.998	0.110	0.045
P3Depth [51]	CVPR'22	0.356	0.898	0.981	0.996	0.104	0.043
NeWCRFs [52]	CVPR'22	0.334	0.922	0.992	0.998	0.095	0.041
AiT [53]	ICCV'23	0.275	0.954	0.994	0.999	0.076	0.033
ZoeDepth [54]	ArXiv'23	0.270	0.955	0.995	0.999	0.075	0.032
<i>Diffusion-based approaches:</i>							
DDP [40]	ICCV'23	0.329	0.921	0.990	0.998	0.094	0.040
VPD [6]	ICCV'23	0.254	0.964	0.995	0.999	0.069	0.030
TADP [7]	ArXiv'23	0.225	0.976	0.997	0.999	0.062	0.027
<b>IEDP (Ours)</b>	-	0.228	0.975	0.997	0.999	0.063	0.027

TABLE III  
IMPACT OF INTEGRATING TWO PROPOSED MODULES INTO THE BASELINE. THE BASELINE ADOPTS SAME ARCHITECTURE AS VPD [6].

Implicit	Explicit	mIoU <sup>SS</sup>	mIoU <sup>MS</sup>
✗	✗	48.1	49.5
✓	✗	49.8	51.1
✓	✓	52.5	53.9

TABLE IV  
IMPACT OF DIFFERENT ADAPTER DESIGN IN IMPLICIT BRANCH. WE EMPLOY AN MLP LAYER OR LEARNABLE QUERIES WITH CROSS-ATTENTION AS THE ADAPTER.

Design	mIoU <sup>SS</sup>	mIoU <sup>MS</sup>
Using an MLP layer	52.1	53.2
Using learnable queries	52.5	53.9

TABLE V  
IMPACT OF DIFFERENT NUMBERS OF LEARNABLE QUERIES. WE SET THE NUMBER OF LEARNABLE QUERIES AS 256.

Number of query	mIoU <sup>SS</sup>	mIoU <sup>MS</sup>
64	51.9	52.4
128	51.5	52.5
256	52.5	53.9

TABLE VI  
IMPACT OF POSITION EMBEDDINGS. WE REPORT THE RESULTS USING POSITION EMBEDDINGS OR NOT IN BOTH IMPLICIT AND EXPLICIT BRANCHES.

Position embeddings	mIoU <sup>SS</sup>	mIoU <sup>MS</sup>
✗	52.3	53.8
✓	52.5	53.9

**Depth estimation.** We compare our proposed method with some state-of-the-art methods on NYUv2 dataset in Table II. These state-of-the-art methods are also divided into classical approaches and diffusion-based approaches. Compared to diffusion-based approaches, our IEDP achieves promising performance. For example, DDP [55] has the RMSE score of 0.329, VPD [6] has the RMSE score of 0.254, and our IEDP has the RMSE score of 0.228. Therefore, compared to DDP and VPD, our IEDP has the relative improvements of 30.7% and 10.2% in terms of RMSE. Compared to TADP [7], our proposed IEDP has a comparable performance, but does not require additional BLIP-2 for generating text prompts.

#### D. Ablation Study

In this section, we will perform detailed analysis to further evaluate the effectiveness of each component in our proposed IEDP. We conduct experiments on semantic segmentation task using ADE20K dataset. We report the results using a fast training strategy with the training iterations of 40K.

**Effectiveness of two proposed modules.** We first perform the ablation study to show the effectiveness of implicit and explicit prompt modules. Table III presents the results of progressively integrating these two modules into the baseline. The baseline

adopts the unaligned text prompts as in VPD [6], which has the mIoU<sup>SS</sup> score of 48.1%. When replacing the unaligned text prompts with our implicit prompts, it has the mIoU<sup>SS</sup> score of 49.8%, outperforming the baseline by 1.7%. When further integrating our explicit prompt module, it has the mIoU<sup>SS</sup> score of 52.5%, which outperforms the baseline by 4.4% totally.

**Different designs of the adapter.** Table IV shows the results of different adapter designs in implicit branch, where the adapter aims to convert the visual features of CLIP image encoder to implicit text embeddings for denoising UNet. We give two different designs, including using an MLP layer and using learnable queries to convert visual features. We observe that using learnable queries has the better performance.

**Number of learnable queries.** Table V shows the impact of different numbers of learnable queries in implicit branch. We observe that there exists a certain degree of performance degradation when using small number of queries, but the decline is relatively limited. Moreover, compared to the baseline, using different queries all have the improvements. We employ the number of queries as 256 as our default setting.

**Impact of position embeddings.** Table VI shows the impact of using position embeddings in both implicit and explicit branch. When not using the position embeddings, it has 0.2%



Fig. 3. **Visualisation results of semantic segmentation.** We provide some qualitative segmentation examples of our proposed method on ADE20K dataset. It can be observed that our proposed method has good segmentation results in various scenarios, including indoor, outdoor, and crowded scene.

TABLE VII  
COMPARISON OF GROUND-TRUTH LABELS AND BLIP-BASED CAPTIONS. IN THE EXPLICIT LANGUAGE GUIDANCE BRANCH, WE EMPLOY GROUND-TRUTH LABELS AND BLIP-BASED CAPTIONS AS TEXT PROMPTS.

Text prompts	mIoU <sup>ss</sup>	mIoU <sup>ms</sup>
Using BLIP generated captions	52.0	52.6
Using ground-truth labels	52.5	53.9

performance drop on mIoU<sup>ss</sup>. Therefore, we add position embeddings in both two branches.

**Ground-truth labels vs. BLIP-based captions.** In explicit language guidance branch, instead of using ground-truth labels, we can also employ BLIP [56] to automatically generate image captions as text prompts like TADP. Table VII compares ground-truth labels and BLIP-based captions. We observe that it has better performance using ground-truth labels that are less noisy.

### E. Qualitative Results

In this subsection we present some qualitative results of our proposed method on both semantic segmentation and depth

estimation tasks.

**Semantic segmentation.** Fig. 3 presents some semantic segmentation examples of our method on ADE20K dataset. Our proposed method presents accurate segmentation results under both indoor, outdoor, and crowded scenes.

**Depth estimation.** Fig. 4 presents some depth estimation examples of our method on NYUv2 dataset. Our proposed method generates accurate depth maps for different indoor scenes, such as bedroom, office, and kitchen.

## V. CONCLUSION

In this paper, we propose an implicit and explicit language guidance framework for diffusion-based visual perception, named IEDP. Our IEDP introduces an implicit prompt module and an explicit prompt module into text-to-image diffusion model. In implicit prompt module, we employ a frozen CLIP image encoder to directly generate implicit text embeddings and fed these embeddings to diffusion model to condition feature extraction. In explicit prompt module, we utilize the ground-truth labels of training images as explicit text prompts and employ CLIP text encoder to generate text embeddings for diffusion model. The implicit prompt module and explicit

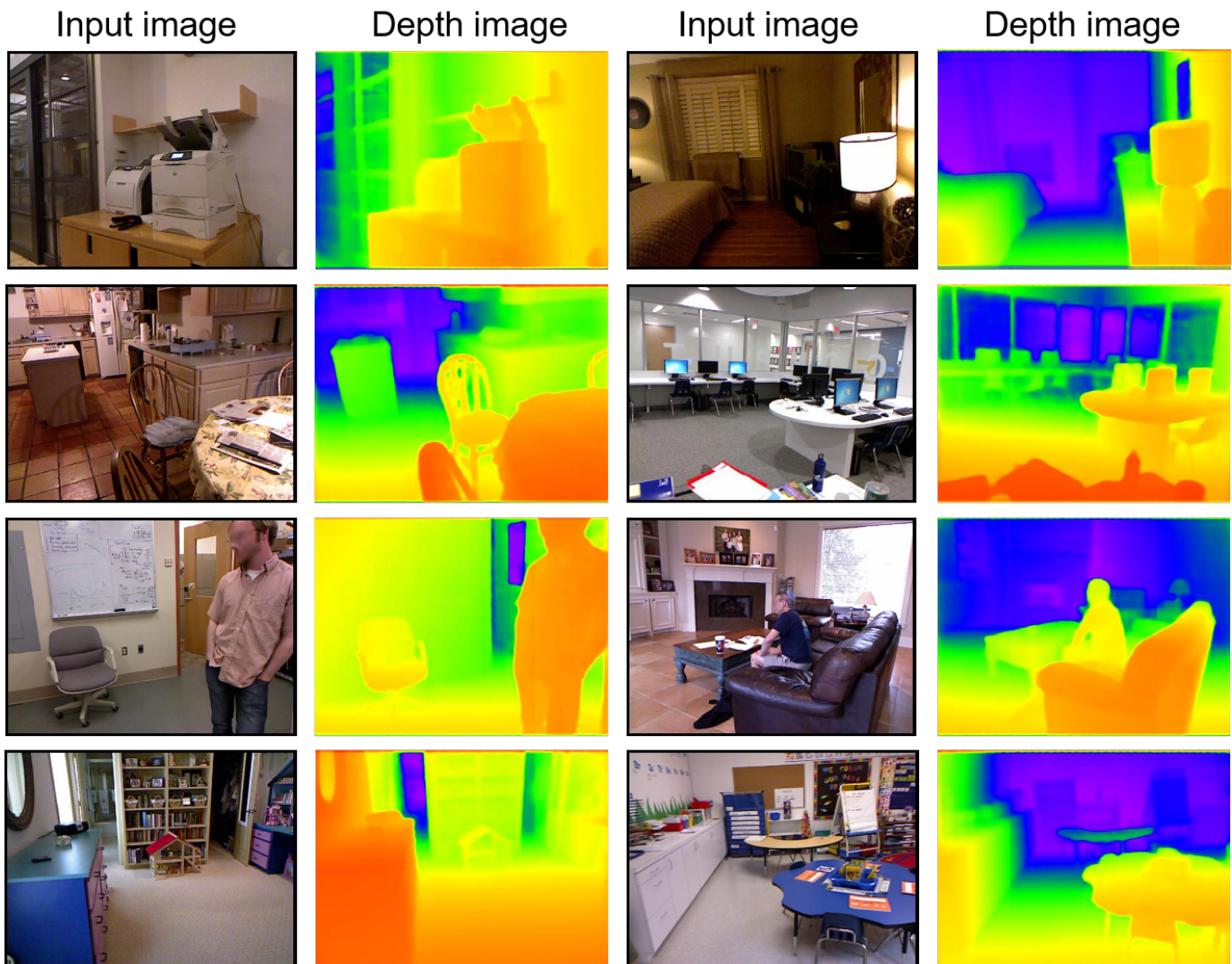


Fig. 4. **Visualisation results of depth estimation.** We provide some qualitative examples of our proposed method on NYUv2 dataset, including the input images and predicted depth maps.

prompt module jointly train the diffusion model, and only implicit prompt module is used during inference. Experiments are performed on semantic segmentation and depth estimation tasks to show the efficacy of proposed method.

#### REFERENCES

- [1] Chitwan Saharia, William Chan, Saurabh Saxena, Lala Li, Jay Whang, Emily L Denton, Kamyar Ghasemipour, Raphael Gontijo Lopes, Burcu Karagol Ayan, Tim Salimans, et al. Photorealistic text-to-image diffusion models with deep language understanding. In *International Conference on Neural Information Processing Systems*, pages 36479–36494, 2022. 1
- [2] Jiahui Yu, Yuanzhong Xu, Jing Yu Koh, Thang Luong, Gunjan Baid, Zirui Wang, Vijay Vasudevan, Alexander Ku, Yinfei Yang, Burcu Karagol Ayan, Ben Hutchinson, Wei Han, Zarana Parekh, Xin Li, Han Zhang, Jason Baldridge, and Yonghui Wu. Scaling autoregressive models for content-rich text-to-image generation. *arXiv preprint arXiv:2206.10789*, 2022. 1
- [3] Aditya Ramesh, Prafulla Dhariwal, Alex Nichol, Casey Chu, and Mark Chen. Hierarchical text-conditional image generation with clip latents. *arXiv preprint arXiv:2204.06125*, 2022. 1
- [4] Robin Rombach, Andreas Blattmann, Dominik Lorenz, Patrick Esser, and Björn Ommer. High-resolution image synthesis with latent diffusion models. In *IEEE/CVF Conference on Computer Vision and Pattern Recognition*, pages 10684–10695, 2022. 1, 2, 3
- [5] Christoph Schuhmann, Romain Beaumont, Richard Vencu, Cade Gordon, Ross Wightman, Mehdi Cherti, Theo Coombes, Aarush Katta, Clayton Mullis, Mitchell Wortsman, et al. Laion-5b: An open large-scale dataset for training next generation image-text models. In *International Conference on Neural Information Processing Systems*, pages 25278–25294, 2022. 1
- [6] Wenliang Zhao, Yongming Rao, Zuyan Liu, Benlin Liu, Jie Zhou, and Jiwen Lu. Unleashing text-to-image diffusion models for visual perception. In *IEEE/CVF International Conference on Computer Vision*, pages 5729–5739, 2023. 1, 2, 3, 4, 5, 6
- [7] Neehar Kondapaneni, Markus Marks, Manuel Knott, Rogério Guimarães, and Pietro Perona. Text-image alignment for diffusion-based perception. *arXiv preprint arXiv:2310.00031*, 2023. 1, 3, 4, 5, 6
- [8] Junnan Li, Dongxu Li, Silvio Savarese, and Steven Hoi. Blip-2: Bootstrapping language-image pre-training with frozen image encoders and large language models. *arXiv preprint arXiv:2301.12597*, 2023. 1
- [9] Alec Radford, Jong Wook Kim, Chris Hallacy, Aditya Ramesh, Gabriel Goh, Sandhini Agarwal, Girish Sastry, Amanda Askell, Pamela Mishkin, Jack Clark, et al. Learning transferable visual models from natural language supervision. In *International Conference on Machine Learning*, pages 8748–8763, 2021. 1



- [10] Ting Chen, Lala Li, Saurabh Saxena, Geoffrey Hinton, and David J Fleet. A generalist framework for panoptic segmentation of images and videos. In *IEEE/CVF International Conference on Computer Vision*, pages 909–919, 2023. 1, 2
- [11] Bolei Zhou, Hang Zhao, Xavier Puig, Sanja Fidler, Adela Barriuso, and Antonio Torralba. Scene parsing through ADE20K dataset. In *IEEE/CVF Conference on Computer Vision and Pattern Recognition*, pages 5122–5130, 2017. 2, 5
- [12] Nathan Silberman, Derek Hoiem, Pushmeet Kohli, and Rob Fergus. Indoor segmentation and support inference from rgbd images. In *European Conference on Computer Vision*, pages 746–760, 2012. 2, 5
- [13] Jonathan Long, Evan Shelhamer, and Trevor Darrell. Fully convolutional networks for semantic segmentation. In *IEEE/CVF Conference on Computer Vision and Pattern Recognition*, pages 3431–3440, 2015. 2
- [14] Hengshuang Zhao, Jianping Shi, Xiaojuan Qi, Xiaogang Wang, and Jiaya Jia. Rethinking atrous convolution for semantic image segmentation. *IEEE/CVF Conference on Computer Vision and Pattern Recognition*, pages 801–818, 2017. 2
- [15] Jiale Cao, Yanwei Pang, and Xuelong Li. Triply supervised decoder networks for joint detection and segmentation. In *IEEE/CVF Conference on Computer Vision and Pattern Recognition*, pages 7392–7401, 2019. 2
- [16] Jingdong Wang, Ke Sun, Tianheng Cheng, Borui Jiang, Chaorui Deng, Yang Zhao, Dong Liu, Yadong Mu, Mingkui Tan, Xinggang Wang, Wenyu Liu, and Bin Xiao. Deep high-resolution representation learning for visual recognition. *IEEE Transactions on Pattern Analysis and Machine Intelligence*, 43(10):3349–3364, 2021. 2
- [17] Liang-Chieh Chen, George Papandreou, Florian Schroff, and Hartwig Adam. Rethinking atrous convolution for semantic image segmentation. *arXiv:1706.05587*, 2017. 2
- [18] Liang-Chieh Chen, George Papandreou, Iasonas Kokkinos, Kevin Murphy, and Alan L Yuille. DeepLab: Semantic image segmentation with deep convolutional nets, atrous convolution, and fully connected CRFs. *IEEE Transactions on Pattern Analysis and Machine Intelligence*, 40(4):834–848, 2018. 2
- [19] Jun Fu, Jing Liu, Haijie Tian, Yong Li, Yongjun Bao, Zhiwei Fang, and Hanqing Lu. Dual attention network for scene segmentation. In *IEEE/CVF Conference on Computer Vision and Pattern Recognition*, pages 3146–3154, 2019. 2
- [20] Zilong Huang, Xinggang Wang, Lichao Huang, Chang Huang, Yunchao Wei, and Wenyu Liu. CCNet: Criss-cross attention for semantic segmentation. In *IEEE/CVF International Conference on Computer Vision*, pages 603–612, 2019. 2
- [21] Yuhui Yuan, Lang Huang, Jianyuan Guo, Chao Zhang, Xilin Chen, and Jingdong Wang. OCNet: Object context for semantic segmentation. *International Journal of Computer Vision*, 129:2375–2398, 2021. 2
- [22] Alexey Dosovitskiy, Lucas Beyer, Alexander Kolesnikov, Dirk Weissenborn, Xiaohua Zhai, Thomas Unterthiner, Mostafa Dehghani, Matthias Minderer, Georg Heigold, Sylvain Gelly, et al. An image is worth 16x16 words: Transformers for image recognition at scale. In *International Conference on Learning Representations*, 2021. 2
- [23] Yuhui Yuan, Rao Fu, Lang Huang, Weihong Lin, Chao Zhang, Xilin Chen, and Jingdong Wang. Hrformer: High-resolution transformer for dense prediction. In *International Conference on Neural Information Processing Systems*, pages 7281–7293, 2021. 2
- [24] Jiaqi Gu, Hyoukjun Kwon, Dilin Wang, Wei Ye, Meng Li, Yu-Hsin Chen, Liangzhen Lai, Vikas Chandra, and David Z. Pan. Multi-scale high-resolution vision transformer for semantic segmentation. In *IEEE/CVF Conference on Computer Vision and Pattern Recognition*, 2022. 2
- [25] Enze Xie, Wenhai Wang, Zhiding Yu, Anima Anandkumar, Jose M. Alvarez, and Ping Luo. Segformer: Simple and efficient design for semantic segmentation with transformers. In *International Conference on Neural Information Processing Systems*, 2021. 2
- [26] Sixiao Zheng, Jiachen Lu, Hengshuang Zhao, Xiatian Zhu, Zekun Luo, Yabiao Wang, Yanwei Fu, Jianfeng Feng, Tao Xiang, Philip HS Torr, et al. Rethinking semantic segmentation from a sequence-to-sequence perspective with transformers. In *IEEE/CVF Conference on Computer Vision and Pattern Recognition*, pages 6881–6890, 2021. 2
- [27] Robin Strudel, Ricardo Garcia, Ivan Laptev, and Cordelia Schmid. Segmenter: Transformer for semantic segmentation. In *IEEE/CVF International Conference on Computer Vision*, pages 7262–7272, 2021. 2
- [28] David Eigen, Christian Puhrsch, and Rob Fergus. Depth map prediction from a single image using a multi-scale deep network. In *International Conference on Neural Information Processing Systems*, pages 2366–2374, 2014. 2, 4
- [29] Dan Xu, Wei Wang, Hao Tang, Hong Liu, Nicu Sebe, and Elisa Ricci. Structured attention guided convolutional neural fields for monocular depth estimation. In *IEEE/CVF Conference on Computer Vision and Pattern Recognition*, pages 3917–3925, 2018. 2
- [30] Shariq Farooq Bhat, Ibraheem Alhashim, and Peter Wonka. Adabins: Depth estimation using adaptive bins. In *IEEE/CVF Conference on Computer Vision and Pattern Recognition*, pages 4009–4018, 2021. 2
- [31] Xiaoxiao Long, Lingjie Liu, Christian Theobalt, and Wenping Wang. Occlusion-aware depth estimation with adaptive normal constraints. In *European Conference on Computer Vision*, pages 640–657, 2020. 2
- [32] Wei Yin, Yifan Liu, Chunhua Shen, and Youliang Yan. Enforcing geometric constraints of virtual normal for depth prediction. In *IEEE/CVF International Conference on Computer Vision*, pages 5684–5693, 2019. 2
- [33] Wei Yin, Jianming Zhang, Oliver Wang, Simon Niklaus, Long Mai, Simon Chen, and Chunhua Shen. Learning to recover 3d scene shape from a single image. In *IEEE/CVF Conference on Computer Vision and Pattern Recognition*, pages 204–213, 2021. 2
- [34] Jonathan Ho, Ajay Jain, and Pieter Abbeel. Denoising diffusion probabilistic models. In *International Conference on Neural Information Processing Systems*, pages 6840–6851, 2020. 2
- [35] Luping Liu, Yi Ren, Zhijie Lin, and Zhou Zhao. Pseudo numerical methods for diffusion models on manifolds. *arXiv preprint arXiv:2202.09778*, 2022. 2
- [36] Cheng Lu, Yuhao Zhou, Fan Bao, Jianfei Chen, Chongxuan Li, and Jun Zhu. Dpm-solver: A fast ode solver for diffusion probabilistic model sampling in around 10 steps. In *International Conference on Neural Information Processing Systems*, pages 5775–5787, 2022. 2
- [37] Jiaming Song, Chenlin Meng, and Stefano Ermon. Denoising diffusion implicit models. In *International Conference on Learning Representations*, 2021. 2
- [38] Shoufa Chen, Peize Sun, Yibing Song, and Ping Luo. DiffusionDet: Diffusion model for object detection. *arXiv:2211.09788*, 2022. 2
- [39] Tomer Amit, Tal Shaharabany, Eliya Nachmani, and Lior Wolf. Segdiff: Image segmentation with diffusion probabilistic models. *arXiv:2112.00390*, 2021. 2
- [40] Yuanfeng Ji, Zhe Chen, Enze Xie, Lanqing Hong, Xihui Liu, Zhaoqiang Liu, Tong Lu, Zhenguo Li, and Ping Luo. Ddp: Diffusion model for dense visual prediction. In *Proceedings of the IEEE/CVF International Conference on Computer Vision*, pages 21741–21752, 2023. 2, 5, 6
- [41] Dmitry Baranchuk, Ivan Rubachev, Andrey Voynov, Valentin Khulkov, and Artem Babenko. Label-efficient semantic segmentation with diffusion models. *arXiv preprint arXiv:2112.03126*, 2021. 3
- [42] Jiarui Xu, Sifei Liu, Arash Vahdat, Wonmin Byeon, Xiaolong Wang, and Shalini De Mello. Open-vocabulary panoptic segmentation with text-to-image diffusion models. In *IEEE/CVF International Conference on Computer Vision*, pages 2955–2966, 2023. 3
- [43] Ze Liu, Yutong Lin, Yue Cao, Han Hu, Yixuan Wei, Zheng Zhang, Stephen Lin, and Baining Guo. Swin transformer: Hierarchical vision transformer using shifted windows. In *IEEE/CVF International Conference on Computer Vision*, pages 10012–10022, 2021. 5
- [44] Zhuang Liu, Hanzi Mao, Chao-Yuan Wu, Christoph Feichtenhofer, Trevor Darrell, and Saining Xie. A convnet for the 2020s. In *IEEE/CVF Conference on Computer Vision and Pattern Recognition*, pages 11976–11986, 2022. 5
- [45] Yongming Rao, Wenliang Zhao, Guangyi Chen, Yansong Tang, Zheng Zhu, Guan Huang, Jie Zhou, and Jiwen Lu. Densclip: Language-guided dense prediction with context-aware prompting. In *IEEE/CVF Conference on Computer Vision and Pattern Recognition*, pages 18082–18091, 2022. 5
- [46] Zhe Chen, Yuchen Duan, Wenhai Wang, Junjun He, Tong Lu, Jifeng Dai, and Yu Qiao. Vision transformer adapter for dense predictions. *arXiv preprint arXiv:2205.08534*, 2022. 5
- [47] Zhenda Xie, Zigang Geng, Jingcheng Hu, Zheng Zhang, Han Hu, and Yue Cao. Revealing the dark secrets of masked image modeling. In *IEEE/CVF Conference on Computer Vision and Pattern Recognition*, pages 14475–14485, 2023. 5
- [48] Jin Han Lee, Myung-Kyu Han, Dong Wook Ko, and Il Hong Suh. From big to small: Multi-scale local planar guidance for monocular depth estimation. *arXiv preprint arXiv:1907.10326*, 2019. 6
- [49] Shariq Farooq Bhat, Ibraheem Alhashim, and Peter Wonka. Adabins: Depth estimation using adaptive bins. In *IEEE/CVF Conference on Computer Vision and Pattern Recognition*, pages 4009–4018, 2021. 6

- [50] René Ranftl, Alexey Bochkovskiy, and Vladlen Koltun. Vision transformers for dense prediction. In *IEEE/CVF International Conference on Computer Vision*, pages 12179–12188, 2021. 6
- [51] Vaishakh Patil, Christos Sakaridis, Alexander Liniger, and Luc Van Gool. P3depth: Monocular depth estimation with a piecewise planarity prior. In *IEEE/CVF Conference on Computer Vision and Pattern Recognition*, pages 1610–1621, 2022. 6
- [52] Weihao Yuan, Xiaodong Gu, Zuozhuo Dai, Siyu Zhu, and Ping Tan. New crfs: Neural window fully-connected crfs for monocular depth estimation. *arXiv preprint arXiv:2203.01502*, 2022. 6
- [53] Jia Ning, Chen Li, Zheng Zhang, Chunyu Wang, Zigang Geng, Qi Dai, Kun He, and Han Hu. All in tokens: Unifying output space of visual tasks via soft token. In *IEEE/CVF International Conference on Computer Vision*, pages 19900–19910, 2023. 6
- [54] Shariq Farooq Bhat, Reiner Birkel, Diana Wofk, Peter Wonka, and Matthias Müller. Zoedepth: Zero-shot transfer by combining relative and metric depth. *arXiv preprint arXiv:2302.12288*, 2023. 6
- [55] Yuanfeng Ji, Zhe Chen, Enze Xie, Lanqing Hong, Xihui Liu, Zhaoqiang Liu, Tong Lu, Zhenguo Li, and Ping Luo. Ddp: Diffusion model for dense visual prediction. *arXiv:2303.17559*, 2023. 6
- [56] Junnan Li, Dongxu Li, Caïming Xiong, and Steven Hoi. Blip: Bootstrapping language-image pre-training for unified vision-language understanding and generation. In *International Conference on Machine Learning*, pages 12888–12900, 2022. 7